

Voltammetric Determination of 6-mercaptopurine at Co(III) Trisphenanthroline Complex and DNA Decorated with Graphene Oxide Modified Glassy Carbon Electrode

Zhihong Yan^{1,2}, Hong Li¹

¹School of Chemistry and Environment, South China Normal University, Guangzhou 510006, PR China.

²College of pharmacy, Guangdong Pharmaceutical University Guangzhou 510006, PR China.

*E-mail: yzhxsp@aliyun.com

Received: 29 July 2015 / Accepted: 20 August 2015 / Published: 26 August 2015

A Cobalt (III) trisphenanthroline complex ($[\text{Co}(\text{phen})_3]^{3+}$) has been adsorption assembled on a glassy carbon electrode (GCE) modified with DNA decorated with graphene oxide (GO) by multiple sweep voltammetry. In the present protocol, GO is served as a functional unit of DNA to greatly improve the efficient immobilization of DNA on the GC electrode and also offer a favorable microenvironment to keep the DNA structure of double-stranded (dsDNA), which facilitates the intercalation of redox-active $[\text{Co}(\text{phen})_3]^{3+}$. The evidences from scanning electron microscope, X-ray diffraction, cyclic voltammetry, electrochemical impedance spectroscopy, emission spectroscopy and differential pulse voltammetry reveal that $[\text{Co}(\text{phen})_3]^{3+}$ can be assembled on the surfaces of GO-decorated dsDNA driven by electrostatic attraction, intercalation and π -stacking interaction. Furthermore, the highly stable $[\text{Co}(\text{phen})_3]^{3+}/\text{GO-dsDNA}/\text{GCE}$ is used to the highly selective determination of 6-mercaptopurine (6-MP) in the human blood with satisfactory. The reduction peak current was linear to 6-MP concentration in the range from 5×10^{-8} to 2×10^{-6} M 6-MP, and the detection limit is 1.5×10^{-8} M ($S/N = 3$)

Keywords: Cobalt (III) trisphenanthroline complex; 6-Mercaptopurine; DNA; Graphene oxide

1. INTRODUCTION

DNA has received particular interest due to its significant biological functions and unique double helix structure, which is exploited as a molecular material of π -electron-rich base pairs [1,2]. Various applications of DNA have been known to be dependent on its synergistic combination with other functional molecules and nanomaterials by different interactions [3–5]. In the recent years, considerable progresses have been acquired to study the interactions of DNA with other molecules by

solution and surface-based electrochemical methods recently [6,7]. A DNA-modified electrode has been developed into the probes of electrochemical biosensors, and applied to investigate the interactions of DNA with other molecules [8,9]. Despite the fact that the use of DNA-modified electrodes has a significant advance, there are still some practical limits, including high cost, low long-term stability and poor reproducibility [10]. With the development of nanoengineering and biotechnology, there have been increasing demands for the efficient preparation of functionalized DNA-modified electrodes [11,12].

Graphene (GR), as a two dimensional (2D) graphitic nanomaterial, has been considered as a promising building block to fabricate single-stranded DNA (ssDNA)-modified electrodes for high-performance electronic devices and electrochemical sensors [13–15]. However, the GR monolayers are stabilized in both aqueous and non-aqueous solvents against aggregation by a relatively large potential barrier, which was main factors that restrict practical application and further development of the GR [16,17]. As one of GR derivatives, graphene oxide (GO) overcomes this drawback. It is heavily oxygenated, comprising hydroxyl and carboxyl groups located at the planar edges, which have devoted to high hydrophilicity and good water dispersibility of GO [18,19]. To date, GO has been used to prepare ssDNA-GO-based functional hybrids, which were highly stable and well dispersible in water, and can be used to fabricate ssDNA-modified electrodes [20–22]. Recently, Xu and co-authors have reported a simple and facile method for the preparation of 3D multi-functional ssDNA-GO hydrogels based on the unwinding of double-stranded DNA (dsDNA) [23]. It is expected to know whether GO with residual π -conjugated systems and functional groups can be used to decorate dsDNA to fabricate high-performance DNA-modified electrodes.

Cobalt(III) trisphenanthroline complexes often have been applied into structural probes of DNA and hybridization indicators of DNA electrochemical biosensors thanks to their excellent redox activity and appropriate π -conjugated planar ligands [24–26]. In addition to the interaction with DNA, this kind of Cobalt(III) trisphenanthroline complexes are able to bind 6-MP, and the 6-MP have been used for the therapy of acute lymphoblastic leukemia [27,28]. On the basis of molecular recognition of the Cobalt(III) trisphenanthroline complexes to 6-MP, the electrochemical techniques have been used for determination of 6-MP [29–31]. However, there is no reports on voltammetric determination of 6-MP employed Cobalt(III) trisphenanthroline complex assembled on GO-decorated dsDNA electrodes.

The purpose of the present work is to fabricate and evaluate of GO-decorated dsDNA electrodes based on electrochemical assembly of $[\text{Co}(\text{phen})_3]^{3+}$, which can be adsorption assembled on the surface of the GO-decorated dsDNA hybrid as schematically in Figure 1. Moreover, the resulting $[\text{Co}(\text{phen})_3]^{3+}/\text{GO-dsDNA}$ modified GCE is used to the highly selective detection of 6-MP in the human blood.

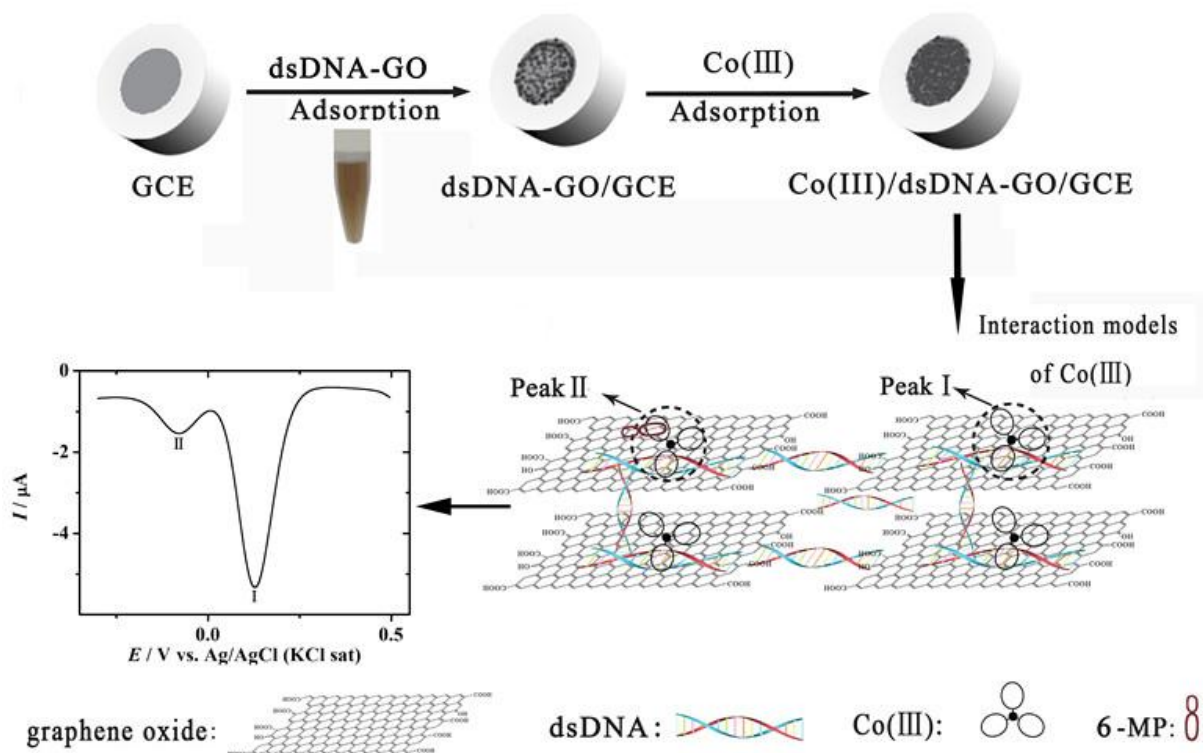


Figure 1. Schematic illustration of the preparation of $[\text{Co}(\text{phen})_3]^{3+}/\text{GO}-\text{dsDNA}/\text{GCE}$ and its voltammetric response to 6-MP ($2 \mu\text{M}$).

2. EXPERIMENTAL SECTION

2.1. Chemicals

$[\text{Co}(\text{phen})_3](\text{ClO}_4)_3$ was synthesized according to the method reported previously [26]. The GO with a thickness of 0.8-1.2 nm and more than 99% high purity was purchased from Nanjing Jicang nano Co. Ltd., China. Tris(hydroxymethyl) aminomethane (Tris) was purchased from Sigma and used to prepare Tris buffer solution, which was composed of 10 mmol L^{-1} Tris and 50 mmol L^{-1} NaCl (pH 7.2). 6-MP (Aladdin Chemistry Co. Ltd., Shanghai, China), methylene blue trihydrate (MB) and herring sperm DNA (dsDNA, Qiyun Co., Guangzhou, China) were applied as received. DNA gave a UV absorbance ratio at 260 nm to 280 nm of 1.89, indicating that the DNA was sufficiently free of protein [32]. Blood was gained by extracting intravenously a healthy volunteer (65 kg) and mixed with the buffer solution at the volume ratio of 1%, 2%, and 3%, designated as samples 1, 2, and 3. All other reagents were of analytical reagent grade and used as received without further purification.

2.2. Instrumentation

Electrochemical experiments were carried out with CHI620d electrochemical working station (Chenhua Instrument Co., Shanghai, China) with a conventional three-electrode system. Which consisted of a bare GCE (EG&G, $\Phi = 3$ mm) or modified GCE working electrode, a titanium plate auxiliary electrode and an Ag-AgCl reference electrode. Fluorescence spectroscopy was performed with a Hitachi RF-2500 fluorescence spectrophotometer (Japan). A Zeiss Ultra55 field emission scanning electron microscope (SEM, Germany) was used to study the surface topography of GO and GO-dsDNA. X-ray diffraction (XRD) patterns were measured on a Bruker-AXS D8 Advance powder x-ray diffractometer (Germany) with Cu K α radiation, and recorded at scanning rate of 0.08 deg s⁻¹ in the 2θ range 5-80°. Electrochemical impedance experiment was performed with an Autolab PGSTAT-30 electrochemical system under open-circuit conditions between 100 kHz and 0.1 Hz with an amplitude of 10 mV. Unless otherwise noted, all the experiments were carried out at room temperature.

2.3. Preparation of GO-DNA modified GCE

Before modification, the bare GCE was polished with 0.3 μ m alumina slurry, and then washed successively with anhydrous alcohol and doubly distilled water in an ultrasonic bath for 10 min and dried in infrared lamp. The GO-dsDNA suspension was prepared by dispersing 1.2 mg GO in 3 mL water containing 15 mg dsDNA with the aid of ultrasonic agitation for 1 h. Next, the GO-dsDNA modified GCE denoted as GO-dsDNA/GCE, was prepared by dropping 8 μ L of GO-dsDNA suspensions onto the GCE surface and dried in air. For comparison, a GO-ssDNA/GCE was prepared using an analogous method with ssDNA-GO, which was prepared by heating the GO-dsDNA suspension in a water bath at 90 °C for 5 min and then allowing it to quickly cool at room temperature [33].

3. RESULTS AND DISCUSSION

3.1. Characterization of GO and GO-dsDNA modified electrodes by SEM and XRD

Figure 1 depicts the idealized scheme for the construction of GO-dsDNA/GCE with a sandwich structure. The dsDNA molecules were bound to two surfaces of GO with many functional groups to form GO-dsDNA hybrid, which contained the negative charges originated from phosphate residues along the polynucleotide chain in a neutral aqueous solution, making the GO exfoliated [34]. As depicted by Figure 2, the wrinkling paper-like GO can be dispersed into thin flakes embedded in the DNA cast film, yielding a GO-decorated DNA electrode.

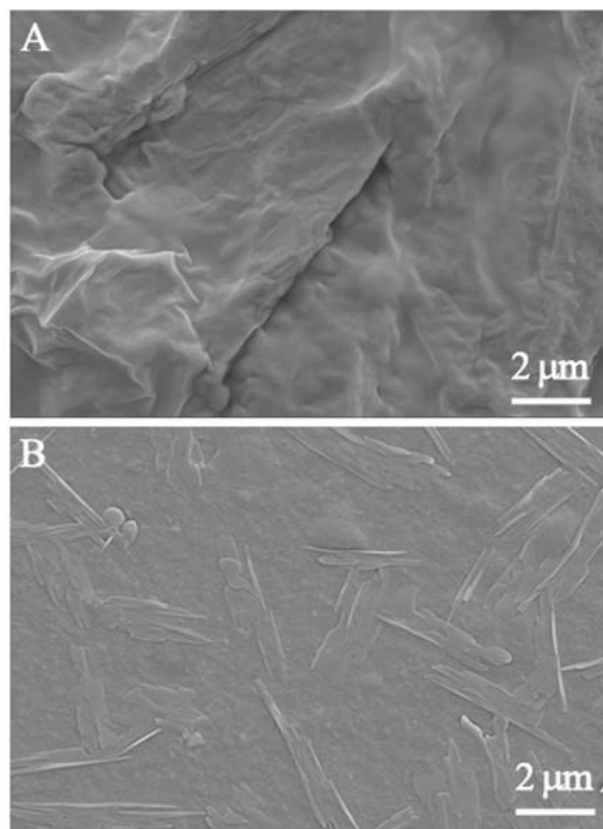


Figure 2. SEM image of GO(A) and GO-dsDNA (B).

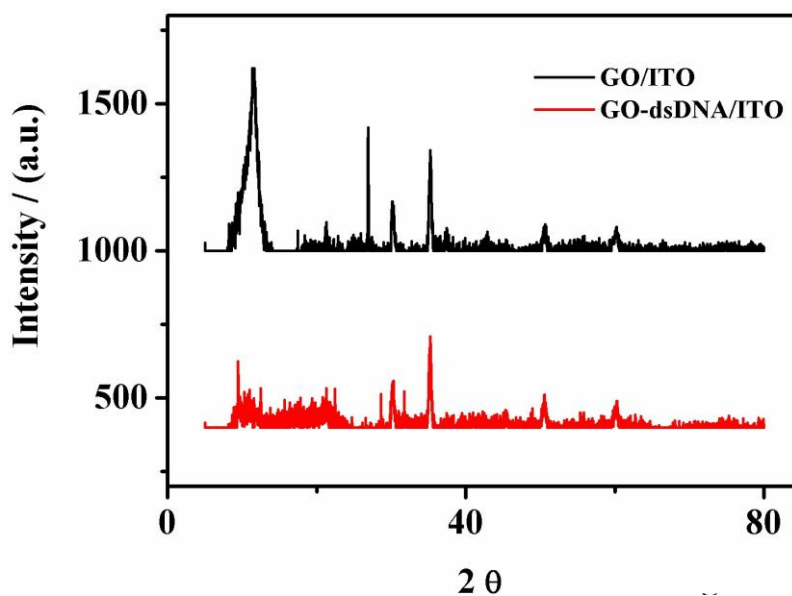


Figure 3. XRD patterns of GO/ITO and GO-dsDNA/ITO.

Figure 3 shows the XRD patterns of GO and GO-dsDNA composites. To better verify the XRD patterns of GO immobilized on the solid electrode, the indium-tin oxide (ITO) was used as the

substrate. The XRD pattern of GO/ITO shows a characteristic peak at $2\theta = 11.4^\circ$ assigned to (002) inter-planar spacing of 0.77 nm [35], and multiple diffraction peaks of ITO [36]. The XRD pattern of GO embedded in the dsDNA film shows that the characteristic peak of GO decreases and even disappears, suggesting that the dsDNA molecules are bound to the two surface of GO, making the layered GO extruded by dsDNA.

3.2. Characterization of GO and GO-DNA modified electrodes by cyclic voltammetry and EIS

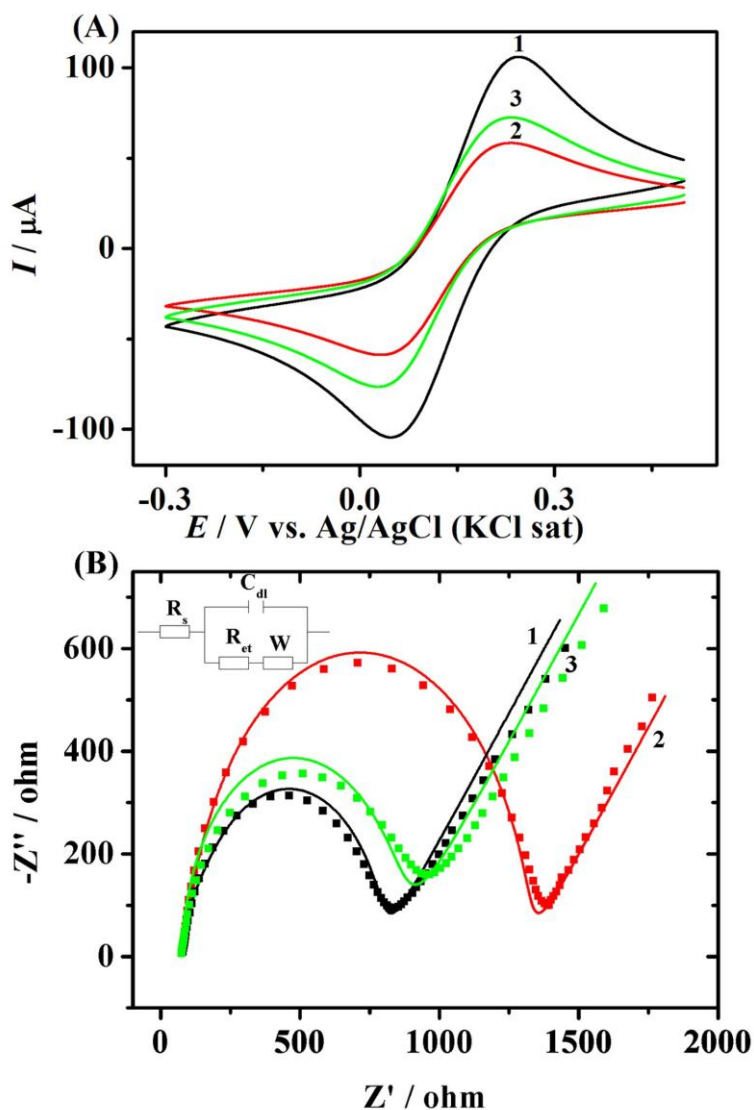


Figure 4. CVs (A, 0.1 V s^{-1}) and Nyquist plots (B, $0.1\text{-}10^5 \text{ Hz}$) of GCE (1), GO-dsDNA/GCE (2) and GO-ssDNA/GCE (3) in $5 \text{ mmol L}^{-1} [\text{Fe}(\text{CN})_6]^{3-/4-}$ ($1:1$)/ $0.1 \text{ mol L}^{-1} \text{ KCl}$. The solid line corresponds to the simulated result with the equivalent circuit depicted by the inset. Note that R_s , C_{dl} , R_{et} and W represent the solution resistance, double layer capacity, electron transfer resistance and Warburg impedance.

Figure 4 gives the cyclic voltammograms (CVs) and Nyquist plots of GO-dsDNA/GCE in 0.1 mol L⁻¹ KCl solutions containing 5.0 mmol L⁻¹ [Fe(CN)₆]³⁻/[Fe(CN)₆]⁴⁻. Compared with the bare GCE, GO-dsDNA/GCE shows the smaller redox peak currents, and larger electron transfer resistance (R_{et}), which is estimated to be 1205 Ω obtained by the equivalent circuit simulation. The result reveals that the negatively charged GO-dsDNA hybrid has been co-assembled on the GCE, making the redox reactions of [Fe(CN)₆]³⁻/[Fe(CN)₆]⁴⁻ with highly negative charges depressed [37]. While unbinding the dsDNA, the redox peak currents and R_{et} values of GO-ssDNA/GCE are between GCE and GO-dsDNA/GCE, suggesting a distinct difference between two DNA-based modified electrodes. The dsDNA bound to GO may keep the double helical structure.

3.3. Electrochemical assembly of [Co(phen)₃]³⁺ on GO-dsDNA/GCE

Figure 5 shows the repetitive CVs of [Co(phen)₃]³⁺ on GO-dsDNA/GCE, revealing a couple of increasing Co(III)/Co(II)-based redox peaks appeared in the 0.05 V and 0.114 V. A peak separation (ΔE_p) of 64 mV indicating that the electrochemical reactions are reversible. In the absence of GO-dsDNA, the redox peaks were not unchanged (curve 1 of Figure 6), suggesting that the presence of GO-dsDNA hybrid leads to an accumulation of [Co(phen)₃]³⁺ on GO-dsDNA/GCE. In the cathodic and anodic potential sweep processes, the positively charged [Co(phen)₃]³⁺ and negatively charged GO-dsDNA are oriented towards the GCE surface, resulting in a redox-active [Co(phen)₃]³⁺/GO-dsDNA/GCE.

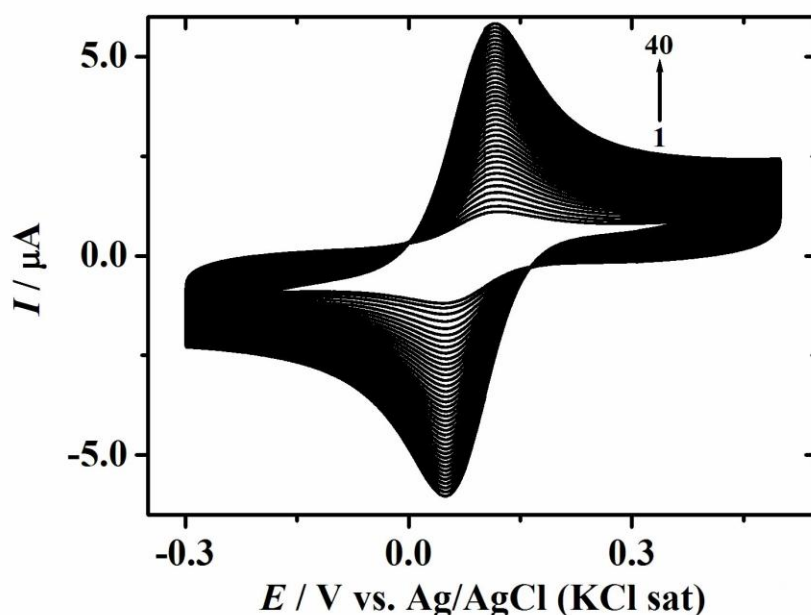


Figure 5. Progressive CVs of 0.2 mmol L⁻¹ [Co(phen)₃]³⁺ on GO-dsDNA/GCE at 0.1 V s⁻¹ scan rate.

To further illustrate the binding interaction between [Co(phen)₃]³⁺ and GO-dsDNA, Figure 6 gives the effects of dsDNA and GO on the redox reactions of [Co(phen)₃]³⁺ on the GCE, which was

known to be controlled by diffusion processes [38]. The addition of dsDNA-GO hybrid leads to a decrease of $[\text{Co}(\text{phen})_3]^{3+}$ -based redox peak currents, suggesting that there exists the strong affinity of GO-dsDNA hybrid to $[\text{Co}(\text{phen})_3]^{3+}$. Figure 7 shows the emission spectra of methylene blue (MB) under the excitation of 595 nm light source, indicating a distinct emission peak at 683 nm (curve 1). While adding the GO-DNA hybrid to the test system, the MB-based excited states are quenched, suggesting an intercalation of MB into dsDNA bound to GO [39]. As further adding $[\text{Co}(\text{phen})_3]^{3+}$, the quenched emission can be restored, revealing that $[\text{Co}(\text{phen})_3]^{3+}$ competes with MB to intercalate into dsDNA bound to GO, making the bound MB free [40].

To sum up, we believe $[\text{Co}(\text{phen})_3]^{3+}$ can be electrochemically assembled on GO-dsDNA surface by electrostatic attraction and intercalation, along with π -stacking interaction between GO and phen ligands.

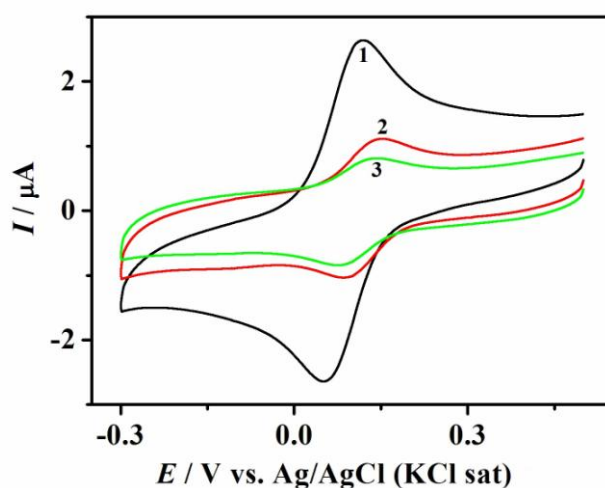


Figure 6. CVs of $0.2 \text{ mmol L}^{-1} [\text{Co}(\text{phen})_3]^{3+}$ in the absence (1) and presence of 5 mg L^{-1} dsDNA (2) and 5 mg L^{-1} dsDNA/ 0.4 mg L^{-1} GO (3) at 0.1 V s^{-1} scan rate.

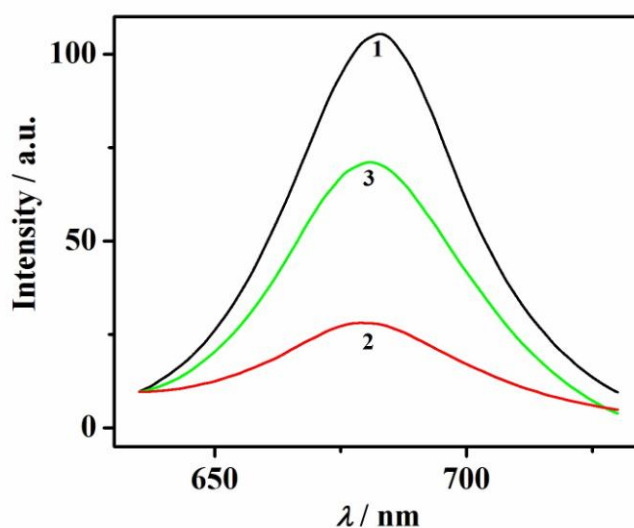


Figure 7. Emission spectra ($\lambda_{\text{EX}} = 595 \text{ nm}$) of 0.01 mmol L^{-1} MB in the absence (1) and presence of 0.5 mg L^{-1} DNA/ 0.04 mg L^{-1} GO (2) and 0.5 mg L^{-1} DNA/ 0.04 mg L^{-1} GO/ 0.02 mmol L^{-1} $[\text{Co}(\text{phen})_3]^{3+}$ (3).

3.4. Electrochemistry of $[\text{Co}(\text{phen})_3]^{3+}/\text{GO-dsDNA}/\text{GCE}$

Figure 8 showed the cyclic voltammograms of $[\text{Co}(\text{phen})_3]^{3+}/\text{GO-DNA}/\text{GCE}$ in the buffer solution with different scan rate. A double of well-defined Co(III)/Co(II)-based redox peaks appeared and the redox peaks current increased gradually with the increase of the scan rate.

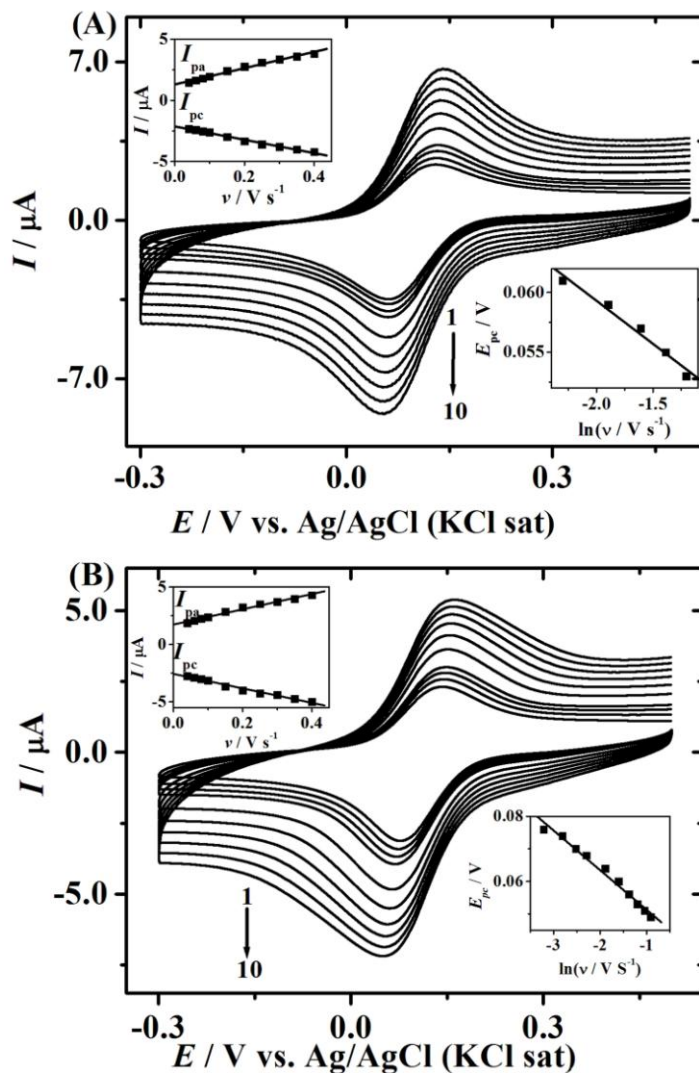


Figure 8. CVs of $[\text{Co}(\text{phen})_3]^{3+}/\text{GO-dsDNA}/\text{GCE}$ (A) and $[\text{Co}(\text{phen})_3]^{3+}/\text{GO-ssDNA}/\text{GCE}$ (B) in buffer solutions at different scan rate (V s^{-1}): (1) 0.04, (2) 0.06, (3) 0.08, (4) 0.10, (5) 0.15, (6) 0.20, (7) 0.25 (8) 0.30 (9) 0.35 and (10) 0.40. Insets show the relations of redox peak currents with scan rate and the cathodic peak potentials with natural logarithm of scan rate.

The redox peaks are of equal height, which increases linearly with increasing scan rate as shown in the inset of Figure 8A (Regression coefficient $R = 0.993$). At 0.1 V s^{-1} scan rate, the formal potential (E°) of $[\text{Co}(\text{phen})_3]^{3+}/\text{GO-dsDNA}/\text{GCE}$ is 0.082 V , taken as an average of the redox peaks potential (which are $E_{p,a}$, 0.114 V and $E_{p,c}$, 0.05 V , respectively,), and the peak separation (ΔE_p) is 64 mV . The results showed that the redox reactions of $[\text{Co}(\text{phen})_3]^{2+}$ on the $\text{GO-dsDNA}/\text{GCE}$ are controlled by a surface-controlled electrochemical process [41]. Combined with the Laviron equation

for diffusionless CVs [42], and the cathodic peak potential ($E_{p,c}$) vs. natural logarithm of scan rate ($\ln v$) plot (inset in Figure 8A), the heterogeneous electron transfer rate constant (k_f) of $[\text{Co}(\text{phen})_3]^{3+}/\text{GO-dsDNA}/\text{GCE}$ is estimated to be 1.65 s^{-1} at $E^{\circ'}$, suggesting a relatively fast electron transfer process [43]. In addition, the cathodic peak height did not change by more than 2.5% after repetitive potential sweep of 40 cycles between 0.50 and -0.30 V , demonstrating high stability of $[\text{Co}(\text{phen})_3]^{3+}/\text{GO-dsDNA}/\text{GCE}$. While the dsDNA-GO hybrid is displaced with ssDNA, the CVs of $\text{GO-ssDNA}/\text{GCE}$ is shown in Figure 8B, indicating a pair of redox peaks at $E^{\circ'} = 0.102 \text{ V}$, which are similar to the CVs of $[\text{Co}(\text{phen})_3]^{3+}/\text{GO-dsDNA}/\text{GCE}$. However, the k_f value of $[\text{Co}(\text{phen})_3]^{3+}$ assembled on $\text{GO-ssDNA}/\text{GCE}$ is 0.47 s^{-1} , which is smaller than that of $[\text{Co}(\text{phen})_3]^{3+}/\text{GO-dsDNA}/\text{GCE}$ due to the long-range electrochemistry-induced electron transfer through the DNA helix [44]. Therefore, $[\text{Co}(\text{phen})_3]^{3+}/\text{GO-dsDNA}/\text{GCE}$ is used to determine the presence of 6-MP as described below.

3.5. 6-MP sensing performances using $[\text{Co}(\text{phen})_3]^{3+}/\text{GO-dsDNA}/\text{GCE}$

Figure 9 shows the DPVs of different concentration 6-MP on $[\text{Co}(\text{phen})_3]^{3+}/\text{GO-dsDNA}/\text{GCE}$. The $[\text{Co}(\text{phen})_3]^{3+}/\text{GO-dsDNA}/\text{GCE}$ shows a $\text{Co}(\text{III})$ -based cathodic peak at 0.112 V (peak I) when it was put into the buffer solution. Upon addition of increasing concentration of 6-MP, as the peak I current continuously decreases, another cathodic peak (peak II) ascribed to the electro-reduction of 6-MP-bound $[\text{Co}(\text{phen})_3]^{3+}$ results in an obvious increase.

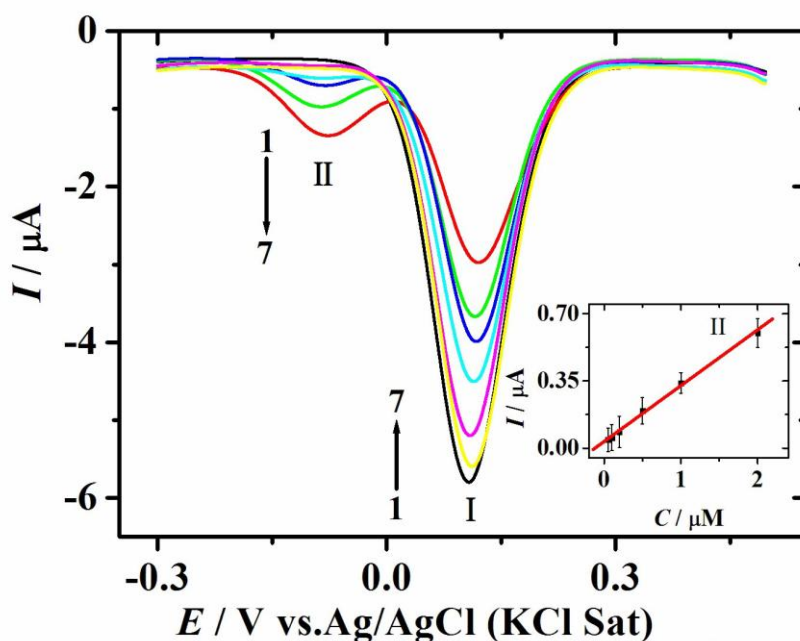


Figure 9. DPVs of $[\text{Co}(\text{phen})_3]^{3+}/\text{dsDNA-GO}/\text{GCE}$ with increasing 6-MP concentration (μM): (1) 0, (2) 0.05, (3) 0.1, (4) 0.2, (5) 0.5 (6) 1.0 and (7) 2.0. Inset: calibration curve of 6-MP.

While making a peak II height vs. 6-MP concentration plot, a linearly increasing voltammetric response to 6-MP is shown as the inset of Figure 9 ($R = 0.997$). The fitted straight line passes through

the origin, and the sensitivity is $0.29 \mu\text{A} (\mu\text{M})^{-1}$ and the detection limit is $0.015 \mu\text{M}$ ($S/N = 3$). The 6-MP sensor based on the $[\text{Co}(\text{phen})_3]^{3+}/\text{GO-dsDNA}/\text{GCE}$ was compared with the reported modified electrodes (Table 1). $[\text{Co}(\text{phen})_3]^{3+}/\text{GO-dsDNA}/\text{GCE}$ has good reproducibility and storage stability. After storing it in refrigerator of 4°C for 15 days the voltammetric response towards 6-MP remains 92.56% of its original value.

Table 1. Comparison of the linear range and detection limit of 6-MP with reported papers

S. no.	Electrode	Linear range (M)	Detection limit (M)	References
1	Multi-wall carbon nanotube modified graphite electrode	0 to 6.67×10^{-2}	1.6×10^{-2}	29
2	Multi-wall carbon nanotube modified glassy carbon electrode	2×10^{-6} to 2×10^{-4}	5×10^{-8}	30
3	Multiwall carbon nanotubes-TiO ₂ modified carbon paste electrode	9×10^{-8} to 3.5×10^{-4}	6.5×10^{-8}	45
4	Silver electrode	2×10^{-7} to 6×10^{-6}	8×10^{-8}	46
5	DNA decorated with graphene oxide modified glassy carbon electrode	5×10^{-8} to 2×10^{-6}	1.5×10^{-8}	This work

3.6. Analytical application in human blood

In order to test the practical application of the method, the 6-MP sensor was used to determine 6-MP in human blood samples. As shown in Table 2, the results of detection showed no 6-MP was discovered in the three samples. Therefore, the standard addition method was adopted in the paper and the recovery of 6-MP is found to be between 98.0 and 103.8%, and the values of the RSD were about 2.3 to 3.2%, suggesting a reliable voltammetric detection method.

Table 2. Determination of 6-MP in the human blood sample

	Added (μM)	Found (μM)	Recovery (%)
Sample 1	10.00	10.10	101
Sample 2	20.00	19.60	98.0
Sample 3	50.00	51.9	103.8

3.7. Reproducibility, Stability and Interference of the 6-MP sensor

The $[\text{Co}(\text{phen})_3]^{3+}/\text{GO-dsDNA}/\text{GCE}$ has good reproducibility. For six electrodes identically, the relative standard deviation (RSD) of the current response to $0.5 \mu\text{M}$ 6-MP was 3.82%. In addition, the storage stability of the 6-MP sensor was also evaluated. After storing it in refrigerator of 4°C for 15 days the voltammetric response towards 6-MP remains 92.56% of its original value, revealing that the sensor had a better stability. $[\text{Co}(\text{phen})_3]^{3+}/\text{GO-dsDNA}/\text{GCE}$ has good selectivity for the detection of 6-MP. 200-fold concentration of K^+ , Ca^{2+} , Mg^{2+} , Fe^{3+} , Al^{3+} , Ni^{2+} , Cl^- , SO_4^{2-} , CO_3^{2-} , PO_4^{3-} , NO_3^- ; 50-fold azathioprine, 6-benzylaminopurine, 6-furfurylaminopurine, zeatin; 10-fold concentration of glucose, lysine, coffein, 6-hypoxanthine, and 5-fold concentration of ascorbic acid, uric acid, dopamine have no influence on the signals of $0.5 \mu\text{M}$ 6-MP with deviations below 5.0%. These performances (reproducibility, stability, selectivity) of the 6-MP sensor is superior to those reported previously [29,30].

4. CONCLUSIONS

In summary, a highly stable redox-active $[\text{Co}(\text{phen})_3]^{3+}/\text{GO-DNA}/\text{GCE}$ has been successfully fabricated based on electrostatic attraction, intercalation and π -stacking interaction between $[\text{Co}(\text{phen})_3]^{3+}$ and GO-DNA hybrid by means of multiple sweep voltammetry. The water-dispersible GO can be served as a functional unit of DNA to greatly improve the efficient immobilization of DNA on the GC electrode and also offer a favorable microenvironment to keep the double helix structure of DNA, which facilitates the intercalation of $[\text{Co}(\text{phen})_3]^{3+}$. The functionalized $[\text{Co}(\text{phen})_3]^{3+}/\text{GO-DNA}/\text{GCE}$ shows an increasing voltammetric response towards 6-MP in the human blood. The present results should be of value for further understanding the interaction between GO-dsDNA hybrid and Co(III) trisphenanthroline complex, as well as offer the outstanding potential to determine the presence of 6-MP.

ACKNOWLEDGEMENTS

This work was supported by the Specialized Research Fund for National Natural Science Foundation of China (No. 21271075) and the Natural Science Foundation of Guangdong Province (No. 10351063101000001).

References

1. S. Ishtiaq, H.L. Thomas, *Nanomedicine and Nanobiotechnology*, 5 (2013) 150–162.
2. J. Sponer, J.E. Sponer, A. Mladek, P. Jurecka, P. Banas, M. Otyepka, *Biopolymers*, 99 (2013) 978–988.
3. Y.M. Hu, X.M. Wang, H.Z. Pan, L.S. Ding, *Bull Chem Soc Ethiop*, 26 (2012) 395–405.
4. K. Cui, Y.H. Song, L. Wang, *Electrochem. Commun.*, 10 (2008) 1712–1715.
5. W.B. Lu, G.H. Chang, Y.L. Luo, F. Liao, X.P. Sun, *J. Mater. Sci.*, 46 (2011) 5260–5266.
6. D. Dasgupta, P. Majumder, A. Banerjee, *J. Biosci.*, 37 (2012) 475–481.

7. L. Fotouhin, Z. Atoofi, M.M. Heravi, *Talanta*, 103 (2013) 194–200.
8. Y.C. Liu, J. Zhao, W.L. Wu, Z.S. Yang, *Electrochim. Acta*, 2 (2007) 4848–4852.
9. E. Mirmomtaz, A.A. Ensafi, S.S. Zad, *Electrochim. Acta*, 54 (2009) 1141–1146.
10. P. Rijiravanich, M. Somasundrum, W. Surareungchai, *Anal. Chem*, 80 (2008) 3904–3909.
11. Y.H. Song, L.L. Wan, Y. Wang, S.C. Zhao, H.Q. Hou, L. Wang, *Bioelectrochemistry*, 85 (2012) 29–35.
12. M. Silvestrini, P. Ugo, *Anal. Bioanal. Chem*, 405 (2013) 995–1005.
13. T. Premkumar, K.E. Geckeler, *Progress in Polymer Science*, 37 (2012) 515–529.
14. S. Alwarappan, K. Cissell, S. Dixit, C.Z. Li, S. Mohapatra, *J. Electroanal. Chem*, 686 (2012) 69–72.
15. W. Lv, F.M. Jin, Q.G. Guo, Q.H. Yang, F.Y. Kang, *Electrochim. Acta*, 73 (2012) 129–135.
16. R. Karthick, M. Brindha, M. Selvaraj, S. Ramu, *Journal of Colloid and Interface Science*, 406 (2013) 69–74.
17. X.F. Zhang, S. Liu, X.N. Shao, *Journal of Luminescence*, 136 (2013) 32–37.
18. X.H. Zhao, Q.J. Ma, X.X. Wu, X. Zhu, *Anal. Chim. Acta*, 727 (2012) 67–70.
19. L.Y. Zhou, Y.J. Jiang, J. Gao, X.Q. Zhao, L. Ma, Q.L. Zhou, *Biochemical Engineering Journal*, 69 (2012) 28–31.
20. W. Li, P. Wu, H. Zhang, C.X. Cai, *Anal. Chem*, 84 (2012) 7583–7590.
21. L.H. Tang, Y. Wang, Y. Liu, J.H. Li, *ACS Nano*, 5 (2011) 3817–3822.
22. O. Akhavan, E. Ghaderi, R. Rahighi, *ACS Nano*, 6 (2012) 2904–2916.
23. K.X. Sheng, Y.X. Xu, C. Li, G.Q. Shi, *Carbon*, 49 (2011) 2878–2881.
24. F. Li, W. Chen, C.F. Tang, S.S. Zhang, *Talanta*, 77 (2008) 1–8.
25. C.F. Ding, F. Zhao, M.L. Zhang, S.S. Zhang, *Bioelectrochemistry*, 72 (2008) 28–33.
26. X.F. He, L. Wang, H. Chen, L. Xu, L.N. Ji, *Polyhedron*, 17 (1998) 316–322.
27. C.F. Zhou, X.S. Du, H. Li, *Bioelectrochemistry*, 70 (2007) 446–451.
28. B.Y. Lu, Y.Y. Lai, H. Li, *Electrochemistry*, 15 (2009) 67–72.
29. B.Y. Lu, H. Li, H. Deng, Z.H. Xu, W.S. Li, H.Y. Chen, *J. Electroanal. Chem*, 621 (2008) 97–102.
30. P.N. Zhou, L.Q. He, G.L. Gan, S.Y. Ni, H. Li, W.S. Li, *J. Electroanal. Chem*, 665 (2012) 63–69.
31. S. Shahrokhian, F.G. Bidkorbeh, A. Mohammadi, R. Dinarvand, *J. Solid. State. Electrochem*, 16 (2012) 1643–1650.
32. M.E. Reichmann, S.A. Rice, A. Thomas, P. Doty, *J. Am. Chem. Soc*, 76 (1954) 3047–3053.
33. Y.X. Xu, Q. Wu, Y.Q. Sun, H. Bai, G.Q. Shi, *ACS Nano*, 12 (2010) 7358–7362.
34. L.H. Tang, Y. Wang, Y. Liu, J.H. Li, *ACS nano*, 5 (2011) 3817–3822.
35. W. Ma, J. Li, B. Deng, X. Zhao, *J. Mater. Sci*, 48 (2013) 156–161.
36. S.R. Ramanan, *Thin Solid Films*, 389 (2001) 207–212.
37. S.F. Liu, J. Liu, X.P. Han, Y.N. Cui, W. Wang, *Biosens Bioelectron*, 25 (2010) 1640–1645.
38. M.T. Carter, A.J. Bard, *J Am Chem Soc*, 109 (1987) 7528–7530.
39. A.P.B. Sinha, C.N.R. Rao, J.R. Ferraro, Academic Press New York 1971, pp. 255–268.
40. D.W. Pang, H.D. Abruña, *Anal Chem*, 70 (1998) 3162–3169.
41. A.J. Bard, L.R. Faulkner, *Electrochemical methods*, Wiley New York, 1980.
42. E. Laviron, *J. Electroanal. Chem*, 101 (1979) 19–28.
43. N.Q. Jia, L.J. Wang, L. Liu, Q. Zhou, Z.Y. Jiang, *Electrochem. Commun*, 7 (2005) 349–354.
44. E.M. Boon, J.K. Barton, *Nucleic acids*, 12 (2002) 320–329.
45. A.A. Ensafi, H.K. Maleh, *Drug Testing and Analysis*, 4 (2012) 970–977.
46. B.Z. Zeng, W.C. Purdy, *Electroanalysis*, 10 (1998) 236–239.